22

Algorithm Selection Based on a Region Similarity Metric for Intracellular Image Segmentation

Satoko Takemoto and Hideo Yokota
Bio-Research Infrastructure Construction Team, RIKEN
Japan

1. Introduction

Live-cell imaging using fluorescence microscopy has become popular in modern biology to analyze complex cellular events such as the dynamics of substances inside cells (Eils & Athale, 2003; Bhaskar & Singh, 2007). The next step in furthering this type of analysis is accumulating useful information from the observed images to quantify the dynamics (Cong & Parvin, 2000; Goldman & Spector, 2004; Harder et al., 2008, Waltera et al., 2010). However, quantification of intracellular images is a difficult process because microscopic images with ultra-high sensitivity have a low signal-to-noise ratio. In addition, the amount of data required for quantification has gradually increased as microscopy has developed. These obstacles make it more difficult for cell biologists to identify regions of interest and accumulate various types of quantitative information, such as the volume, shape, and dynamics of intracellular substances. Hence, it is important to develop computational methods for identifying objective targets, such as organelles labeled with, for example, a fluorescent protein.

Image segmentation, the process by which an image is divided into multiple regions corresponding to the components pictured in the image, plays a key role as one of the first steps in the quantification of objective targets from observed images. The use of segmented regions allows us to distinguish substances of interest from irrelevant regions, including background and noise. Numerous segmentation algorithms have been proposed (e.g., Haralick & Shapiro, 1985; Pal & Pal, 1993), but most approaches have been developed for a specific task and cannot be generalized for other segmentation tasks. As a result, researchers have had to face the difficult duty of choosing the most suitable algorithm for a given task while facing increasing numbers of images needing quantification. Moreover, recent notable improvements in live-cell imaging require that segmentation algorithms be flexible enough to accommodate time-variable changes in targets. No single algorithm performed with a fixed-parameter setting is considered to be sufficient for analyzing all time-lapse images, and optimizing algorithms for a variety of images is a tedious task for researchers.

Solutions to these problems have been proposed based on the idea of algorithm selection (e.g., Cardoso & Corte-Real, 2005; Zhang, 2006; Polak et al., 2009). An appropriate algorithm with an optimized parameter setting for each task is automatically selected according to unique evaluation metrics of algorithm performance. Evaluation can be roughly divided into two types: unsupervised evaluation and supervised evaluation. The former type can

evaluate different algorithms only by simply computing some chosen evaluation metrics without requiring a prior knowledge about segmentation targets (Cardoso, 2005; Zhang et al., 2006). Statistical features, such as the grey-level standard deviation or homogeneity of pixel intensities in the segmented region, are generally computed. For example, a region contrast (Levine & Nazif, 1985) or region shape (Sahoo et al., 1988) have been proposed (see the comprehensive survey; Zhang et al., 2008). Although the advantage of unsupervised evaluation is that a large number of segmentation algorithms can be evaluated, if there is no guarantee that the pre-defined range for some statistical features will be satisfied, unsupervised evaluation should not be used. In addition, the range of features of intracellular substances cannot be pre-defined, and the diversity in features of intracellular substances may destabilize the result of evaluation.

The latter type can evaluate different algorithms by using some metrics based on similarity (or error) measurement between two regions: an automatically segmented region and a manually segmented region, called the reference region or the ground-truth (e.g., Zhang & Gerbrands, 1992; Martin et al., 2001; Jiang et al., 2006; Polak et al., 2009). For example, the number of mis-segmented pixels (Ysnoff et al., 1977), or the number of segmented targets (Zhang, 1996) is commonly used as an error measurement. Although metrics for supervised evaluation have been proposed so as to reflect the human perception, it is not clear whether the evaluation procedure has actually reflected the perception. That is, the region, which is segmented by using the selected algorithm, may not identify the objective targets to be quantified.

In this research, we propose a novel evaluation metric composed of similarity measurements of a combination of intensity-based and shape-based image features between a segmented region and the ground-truth. Our evaluation metric adopts the philosophy of supervised evaluation and expands it so as to reflect the human perception. We chose these two kinds of image features because cell biologists usually pay attention to them when identifying objective targets, and our proposed method is able to select an appropriate algorithm with optimal parameter settings so as to satisfy biologists' intentions.

The proposed method evaluates the performance of segmentation algorithms by comparing each segmentation result with the ground-truth specified by cell biologists, and it predicts which algorithm will provide the best performance on new images that have similar image features to the original ground-truth. We investigated the performance of two types of segmentation algorithms under our proposed evaluation metric for the identification of fluorescent labeled targets with granular shapes on real intracellular images. In addition to demonstrating the automatic selection of an appropriate algorithm suited to the segmentation task, we showed that our evaluation metric can rank different types of algorithms. We also tested to see whether the selected algorithm showed good segmentation results for other similar images.

The rest of the paper is structured as follows. In Section 2, we describe the algorithm selection framework and explain our proposed evaluation metric based on the region similarity. Experimental results and discussion including segmentation quality for intracellular images taken by a confocal microscope are presented in Section 3. Finally, a conclusion is offered in Section 4.

2. Algorithm selection framework

Many possible solutions must be considered when establishing a segmentation algorithm for a specific application that satisfies a user's intention. In many cases, a target intracellular

substance can be represented by a homogeneous unique image feature and can be distinguished from other substances, even from background. Here, we focus on the segmentation techniques implemented by a pattern classification technique (Duda et al., 2007) that can classify image features into classes (or categories) associated with substances. When performing segmentation, the computer first calculates *N*-dimensional image features that are derived by pixel intensity and classifies them into multiple classes in the *N*-dimensional feature space. Ideally, each class is associated with one substance pictured in the image, such as an organelle in intracellular images. In the case of supervised classification, the distribution of image features of each class is initially specified by a user who has knowledge of the segmentation target. Then the classifier (i.e. classification rule), such as a discriminant function, is generated based on their distribution so as to assign the image features to a specified class. Manual segmentation is generally conducted for specifying classes. According to the generated classification rule, the computer is able to automatically classify the new inputs that are calculated from the still unsegmented images. As a result, target segmentation can be achieved by detecting only the pixels that have the feature classified as the target class (see Fig. 1).

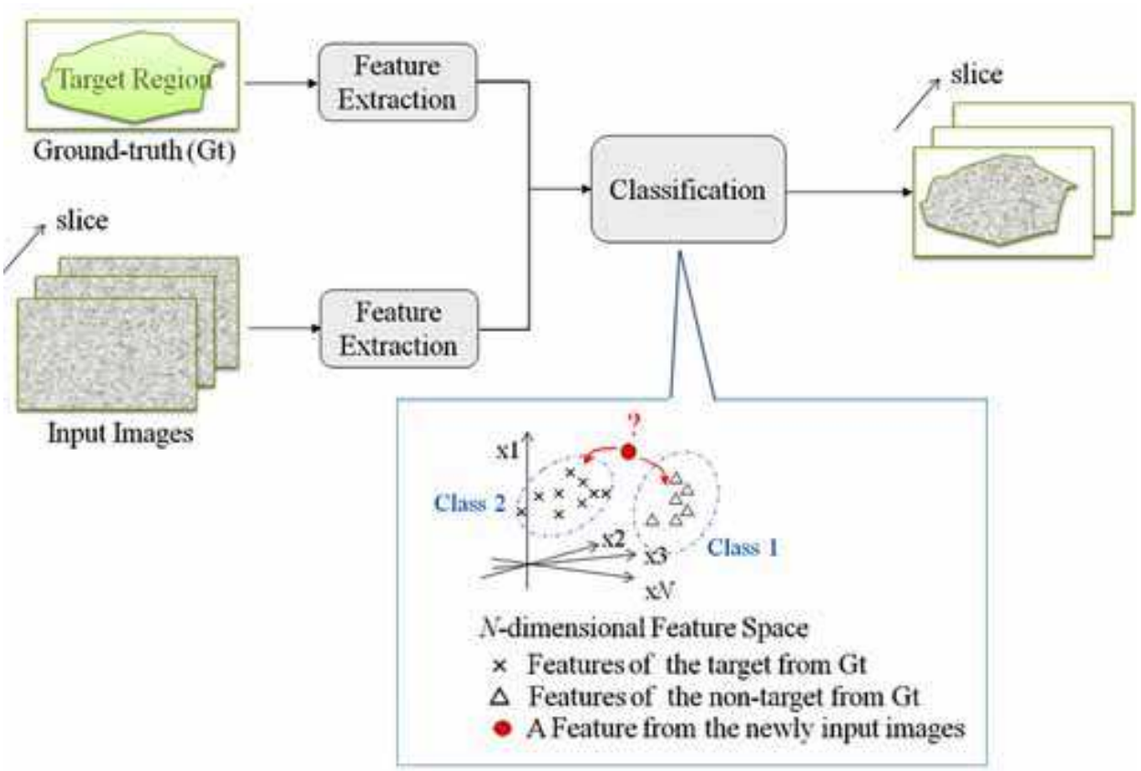

Fig. 1. A segmentation approach based on pattern classification theory. In this approach, the user specifies the region of the segmentation target.

However, the segmentation algorithm implemented by this classification technique is not general enough because there will be large differences in segmentation results depending on the algorithm used. That is, the segmentation results are greatly influenced by the type of features and classification rules adopted, and the optimal algorithm for one segmentation

task may not be optimal for a different one. To solve these problems, we propose a new framework that can select an optimal algorithm that satisfies the user's intention in each segmentation task.

Here, "algorithm" means the set including the feature space constructed by the extracted image feature, the classification rule, and the parameter settings for generating the feature space and the classification rule. Our framework selects the algorithm that can extract the target region with the highest level of accuracy by means of our proposed evaluation metric, as long as the ground-truth is specified. As shown in Fig. 2, the algorithm that can segment the region most similarly to the ground-truth is automatically selected from a given set of algorithms.

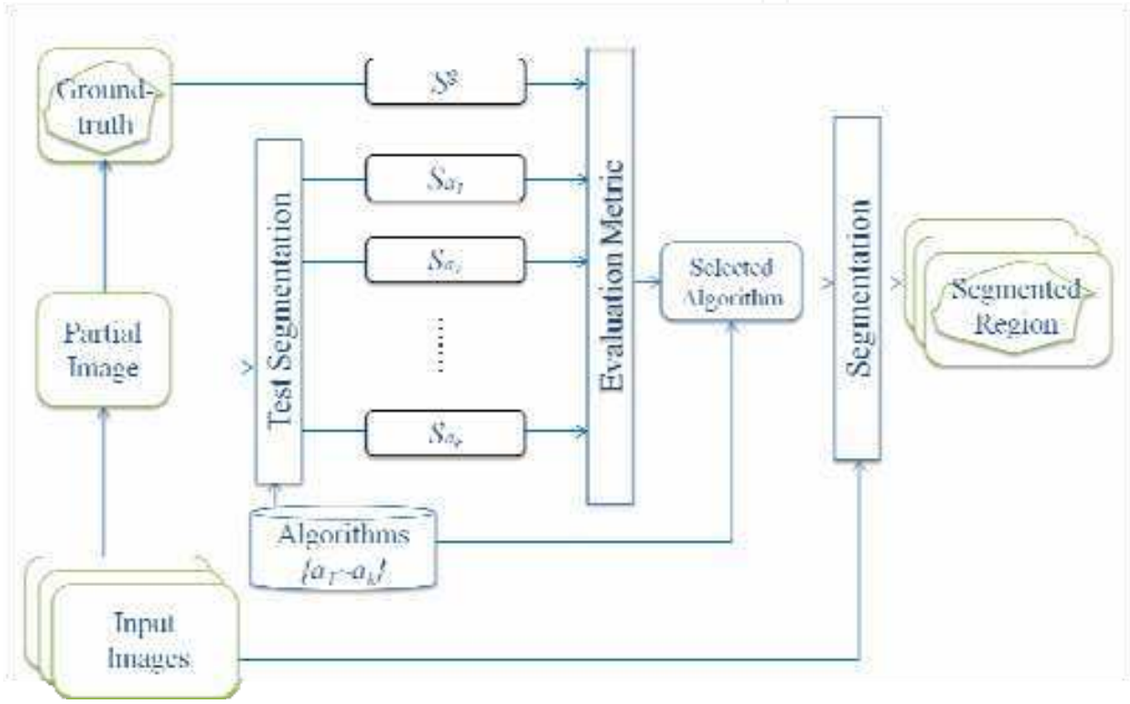

Fig. 2. A framework of algorithm selection.

2.1 Selection metric

The similarities between the ground-truth and the automatically segmented region produced by each given algorithm are used as an evaluation metric for selecting the proper algorithm in our framework. Previous researchers have used many evaluation metrics based on similarities with the ground-truth. For example, (Haindl & Mikes, 2008; Arbelaez, 2009) considered segmentations as a clustering of pixels, and used the Variation of Information (VI), which is based on the distance between two clusters in terms of their average conditional entropy, to measure similarity between two segmentations. Similarly, (Unnikrishnan et al., 2007) introduced the Rand Index (RI) for measuring the distance of two clusters by comparing the compatibility of assignments between pairs of elements in the clusters. Although it is possible to evaluate the performance of segmentation algorithms using the RI and VI and the number of segmented regions evaluated is not constrained with these indexes, their perceptual meaning (that is, an association between human judgement

and these indexes) and applicability in the presence of the ground-truth reference (i.e., supervised evaluations) remains unclear.

Martin et al. (Martin et al., 2001) proposed the similarity indexes called Global Consistence Error (GCE) and Local Consistent Error (LCE), which are well-known as evaluation metrics for natural image segmentation. Although there are limitations in terms of the number of segmented regions that can be evaluated and computational cost, a notable advantage of these metrics is that supervised evaluation based on human perception can be conducted only from the viewpoint of region boundaries.

Our evaluation metric for intracellular image segmentation is composed of similarity measurements between the ground-truth and automatically segmented regions, not only from the viewpoint of region boundaries but also from the statistical features in the segmented region. The similarity is measured by the distance of the intensity-based and the shape-based image features between the two regions. The algorithm that produces the minimum distance is defined as the optimal one for a given segmentation task. That is, a user can obtain the most accurate segmentation result by using the selected algorithm to segment a target that has similar characteristics to the ground-truth. It is well known that, if a highly accurate identification is achieved for a feature distribution with a certain classification rule (e.g., a discriminant function), the rule is also applicable to a similar feature distribution and can lead to accurate classification results (Duda et al., 2007).

People generally focus on specific characteristics of a region when evaluating a segmented region. We consider that image features derived from the pixel intensity and boundary shape of the segmentation target are the most important characteristics. We defined S^g as the target region of the ground-truth that is supervised by a user and $S=\{S_a, a\in A\}$ as the automatically segmented regions by given algorithms in a plane (or a space). The similarity R_A between those two regions can be calculated as follows:

$$R_A = \frac{1}{dist(S^g, S)} = \frac{1}{dist(\mathbf{X}^g, \mathbf{X}_A) + dist(\mathbf{P}^g, \mathbf{P}_A)}, \tag{1}$$

where $\mathbf{X}=(x_1, x_2, ..., x_N)$ represents the N-dimensional image features and $\mathbf{P}=(p_1, p_2, ..., p_n)$, $(p_j \in C^N)$ represents the spatially discrete shape features of a region. The symbol $dist(\cdot)$ means the distance calculation of two elements. That is, R_A is defined as a linear combination of $dist(\mathbf{X}^g, \mathbf{X}_A)$ and $dist(\mathbf{P}^g, \mathbf{P}_A)$. We can select an optimal algorithm that can segment a similar region with the ground-truth as follows:

$$a_i = \arg \min_{0<i\le k} \frac{1}{R_{a_i}} \tag{2}$$

where k is the number of given algorithms. The feature derived from pixel intensity, such as texture, differential features, or local correlation, is set to $\mathbf{X}$. In our framework, we measure $dist(\mathbf{X}^g, \mathbf{X}_A)$ by using the Bhattacharyya distance, which is an approximate measurement between two statistical distributions.

2.2 Discrete description of boundary shape

To calculate the shape-based image feature $\mathbf{P}$, we use the set of boundary points (x_j, y_j) $(j=0, 1, ..., M-1)$ obtained by sampling sequential boundary pixels to describe the

shape of the target region. A complex autoregressive model is applied to these boundary points, and this leads to a stable shape description invariant to translation, rotation, and scale of patterns (Sekita et al., 1992). First, each boundary point is represented by a complex number $z_j = x_j + iy_j$ (see Fig. 3).

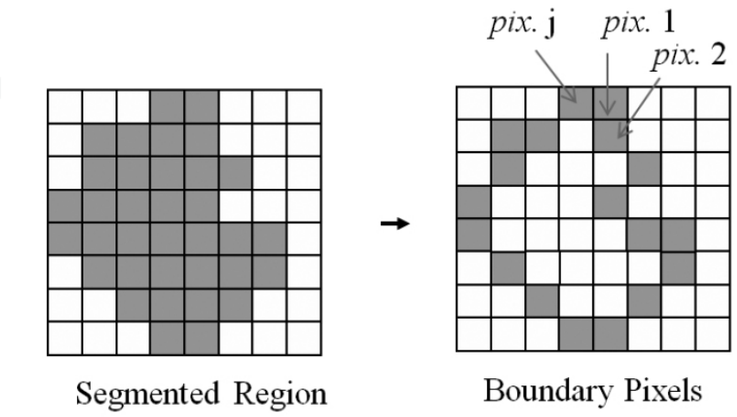

	x	y
pix. 1	3	0
pix. 2	4	0
pix. 3	2	1
.	.	.
.	.	.
pix. j	x_j	y_j

x-y coordinates of the Boundary Pixels

	z
pix. 1	$3 + 0\,i$
pix. 2	$4 + 0\,i$
pix. 3	$2 + 1\,i$
.	.
.	.
pix. j	$x_j + y_j\,i$

Complex Representation

Fig. 3. Schematic diagram of the boundary shape description.

Next, the complex autoregressive model can be applied to each boundary point, which can be represented by a linear combination of the preceding m boundary points as follows:

$$\hat{z}_j = \sum_{k=1}^{m} b_k z_{j-k}, \tag{3}$$

where $\{b_k\}_{k=1}^{m}$ is defined by minimizing the mean squared error of $\varepsilon^2(m)$, which can be calculated as follows:

$$\varepsilon^2(m) = \frac{1}{M} \sum_{j=m}^{M-1} (\hat{z}_j - z_j)^2. \tag{4}$$

According to these definitions, the distance between the two boundaries $z^{(n)} \in C^N, (n \in \{1, 2\})$ can be defined as follows:

$$Db(1,2) \equiv \sqrt{\sum_{k=1}^{m} \left| b_k^{(1)} - b_k^{(2)} \right|^2} . \quad (5)$$

That is, the distances represented in Eq. (5) are defined as the Euclidean distance of each coefficient b_k represented in Eq. (3). For example, the distance between boundary shape S_0 and its deformed shape S_1 is 52.99 and that between S_0 and its deformed shape S_2 is 36.78 (see Fig. 4). The difference between S_0 and S_2 is less than that between S_0 and S_1, so the boundary shape of S_2 is more similar to the shape of S_0 than is the boundary shape of S_1. We use this similarity measure to evaluate whether the automatically segmented region is similar to the supervised region.

Fig. 4 Examples of a boundary shape (left, S_0) and two deformed shapes (centre, S_1; right, S_2).

3. Validation on confocal microscope images

Various types of organelles (e.g., nuclei and mitochondria) and cytoskeletons (e.g., actin and tubulin) exist in cells, and they can be roughly grouped as having granular shapes, fibrous structures, mesh structures, or other similar features. As a preliminary test of the algorithm selection for segmenting substances that have granular shapes, we used the Golgi apparatus region marked by a fluorescent protein from botanical yeast images as a segmentation target. Figure 5a shows the image taken under a confocal microscope, and Figure 5b shows the specified target region by a biologist, that is, the ground-truth. In this test, we evaluated

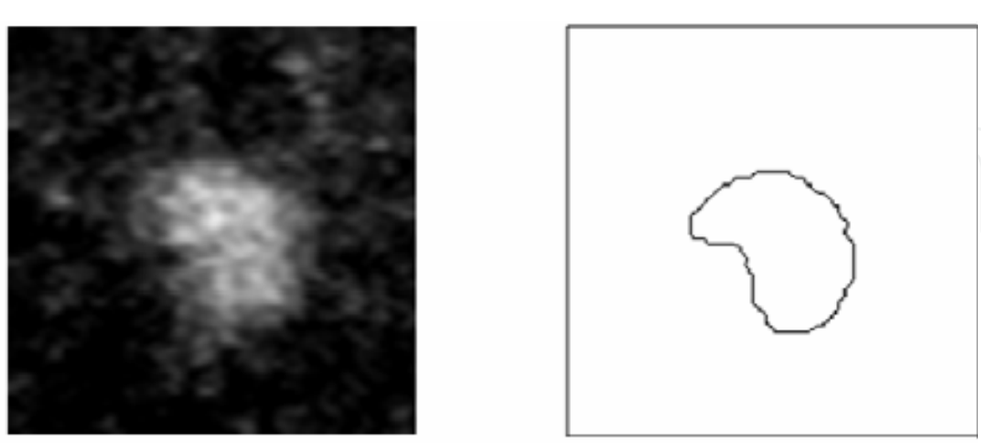

(a) Original Image (b) Ground-truth

Fig. 5. Experimental images. The line in (b) is the manually specified boundary of the segmentation target of the original image (a).

whether the given algorithms were able to extract the target region with a high degree of similarity to the ground-truth from the viewpoint of the previously discussed metric.
The test segmentation was first conducted for the entire group of multiple given algorithms; therefore, there was the same number of segmentation results as algorithms. Next, for all the segmentation results, we calculated the intensity-based image features inside the automatically segmented region and described the region's boundary shape numerically by the methods described in Section 2.2. At the same time, we calculated the intensity-based image features of the target region of the ground-truth and described its boundary shape numerically. Finally, we computed the similarity between the ground-truth and each automatically segmented region by Eq. (1).
Although numerous methods for extracting intensity-based image features can be applied in our framework, we used the two types of image features associated with each pixel as a prototype in this preliminary test: normalized pixel intensity and texture-based statistics inside the local region in which each pixel is centrally positioned. The latter is calculated as follows:

$$X_{pq} = \sum\sum m^p n^q f(m,n), \tag{6}$$

where m and n are the x-y coordinates inside the image, and $f(m,n)$ is the local region consisting of a 5×5 set of pixels. These calculated features are equivalent to moments, and in this test, we calculated the normalized moment of order 2 around (m,n) as the second image feature.
The Support Vector Machine (SVM) (Vapnik, 1995) and Approximate Nearest Neighbour (ANN) (Arya et al., 1994) were defined as classification rules in this test, and some parameters had to be set for each classification rule. We defined three types of parameter settings (P1–P3) related only to the kernel functions in SVM and two types of parameter settings (P4 and P5) related only to the number of nearest neighbours in ANN. The combination of features, classification rules, and parameters produced the 10 segmentation algorithms shown in Table 1. In this table, F1 shows the feature derived from pixel intensity, F2 shows the feature derived from texture-based statistics, M1 is SVM, and M2 is ANN.
Figure 6 shows the distance of intensity-based feature distribution between the ground-truth and each segmented region for each algorithm. Similarly, Figure 7 shows the shape

Algorithm Number	Feature	Classification Rule	Parameter-setting
A1	F1	M1	P1
A2	F1	M1	P2
A3	F1	M1	P3
A4	F2	M1	P1
A5	F2	M1	P2
A6	F2	M1	P3
A7	F1	M2	P4
A8	F1	M2	P5
A9	F2	M2	P4
A10	F2	M2	P5

Table 1. The 10 experimental algorithms.

distance between them. After normalizing each distance, the similarities were computed by Eq. (1), and the results indicate that the segmented region of A4 was most similar to the ground-truth (Table 2). Therefore, we regard A4 as the most proper segmentation algorithm, not only for this task but also for similar tasks, as long as the target has similar characteristics to the ground-truth.

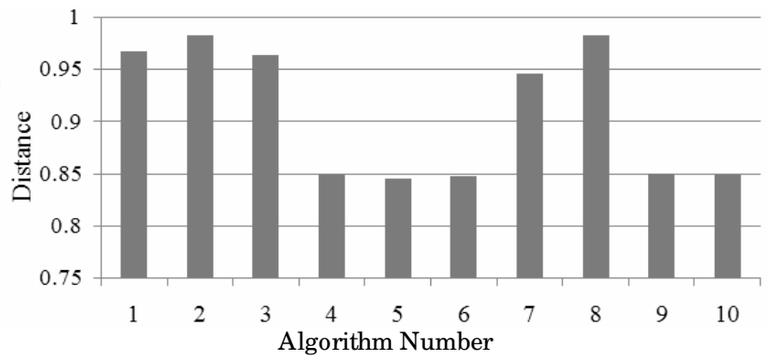

Fig. 6. Distance between the results of A*i* and the ground-truth for the intensity-based image features.

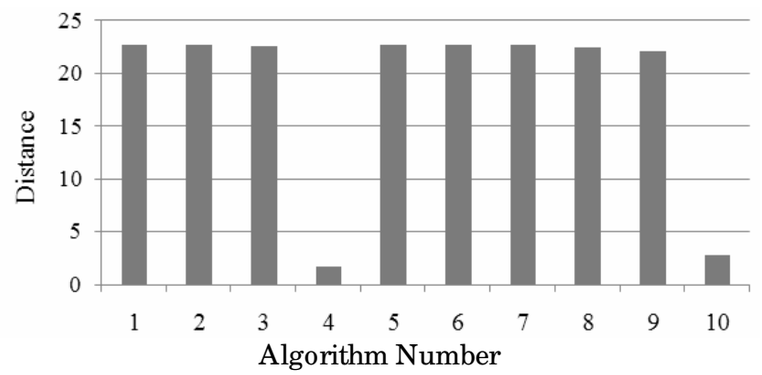

Fig. 7. Distance between the results of A*i* and the ground-truth for the shape-based image features.

Algorithm Number	Normalized Similarity	Performance Ranking
A1	1.48	8
A2	1.73	10
A3	1.41	7
A4	-3.05	1
A5	-0.52	3
A6	-0.49	5
A7	1.13	6
A8	1.70	9
A9	-0.50	4
A10	-2.91	2

Table 2. Performance ranking of the algorithms by our evaluation metric.

Figure 8 shows the target regions segmented automatically by using each algorithm; it is clear that several results include isolated regions other than the target region. In those cases, we calculated the distance on the basis of only the largest region. For comparison, we also show a binarization result provided by the Otsu method (Otsu, 1979) as A11. Because the original image was extremely noisy, the binarization result contained false positive errors. Algorithm A4, however, was not affected by the noise and achieved a highly accurate segmentation.

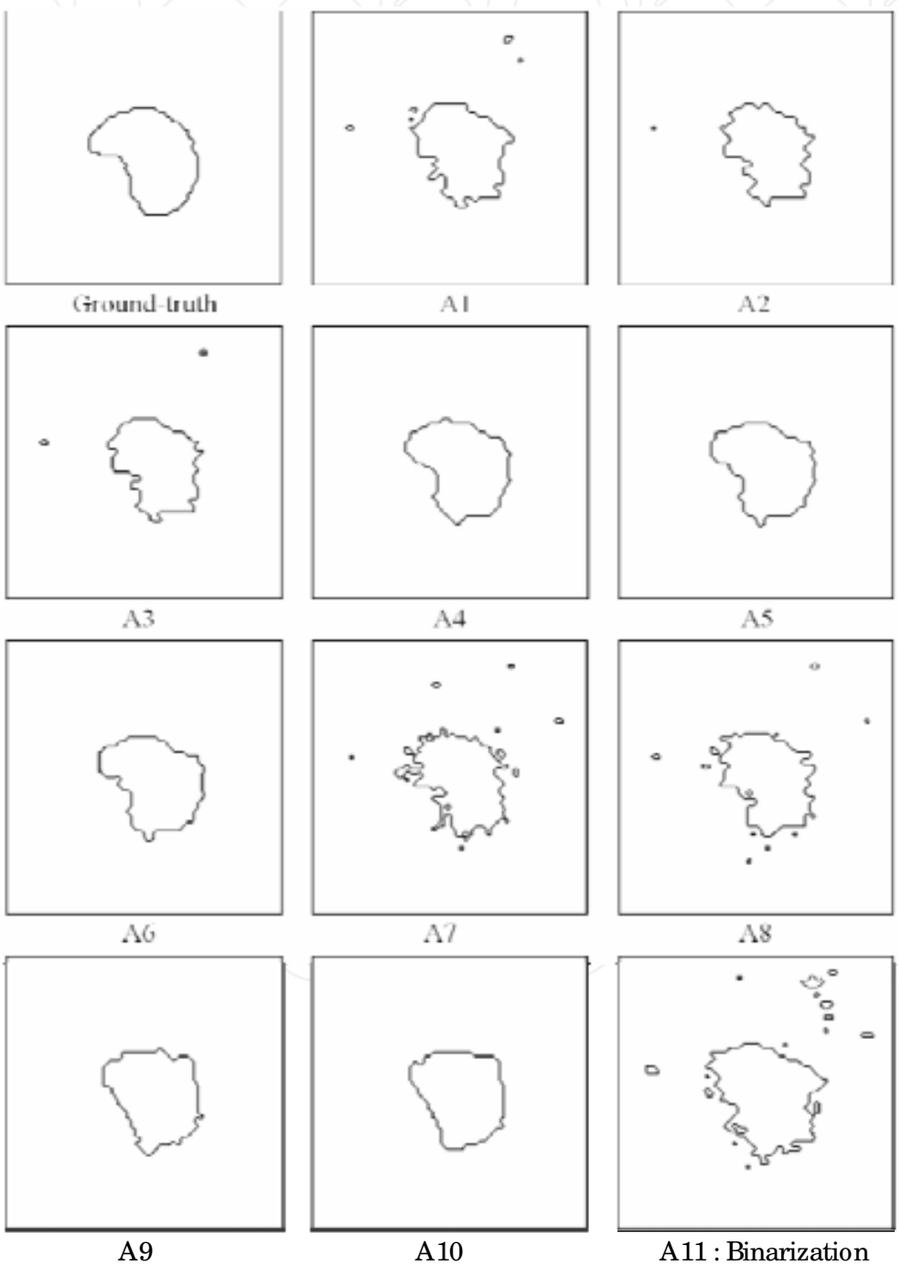

Fig. 8. Segmentation results for all the algorithms. A4 was determined to be the optimal algorithm

If we had used only the metric derived from the intensity-based image features, A4, A5, A6, A9, and A10 could have been selected as the proper algorithm. Similarly, if we had used only the metric derived from the shape-based image features, A4 or A10 could have been selected. However, as can clearly be seen in Fig. 8, over-segmentation occurs in A9 and A10. Because we used a combination of two metrics based on the image features in the evaluation function in Eq. (1), we avoided the risk of choosing a suboptimal algorithm.

In addition, although A4-A6 in Fig. 8 appear to be similar to each other, there is a large difference in the boundary shape when A4 is compared with A5 and A6 (see Fig. 7), especially for the biologists. In the segmented images of A4-A6, the centre-left of each segmented region clearly has a larger boundary change than the other regions. Although false-negative error occurs in that region in A5 and A6, A4 achieved an accurate segmentation reflecting the boundary of the ground-truth (see Fig. 8). Our evaluation function did not miss the difference between these results, which appears to be biologically important. Even if the differences were trivial, however, the evaluation framework was able to select the most proper algorithm to reflect the biologist's intention.

We conducted a similar test to validate the conventional evaluation metric. GCE proposed by Martin et al. (Martin et al., 2001) was used as an example of typically supervised evaluation metric. Evaluation for the same images shown in Fig. 8 according to GCE is summarized in Table 3. Although more data are required to validate the advantage of our proposed evaluation metric, GCE was not able to select A4 as the most proper algorithm for this segmentation task in this validation test.

Algorithm Number	Global Consistency Error	Performance Ranking
A1	0.01326	10
A2	0.01321	8
A3	0.01323	9
A4	0.01181	3
A5	0.01145	2
A6	0.01193	4
A7	0.01315	6
A8	0.01318	7
A9	0.01196	5
A10	0.01129	1

Table 3. Performance ranking of the algorithms by GCE (Martin et al., 2001).

Our segmentation framework assumes that images having similar characteristics will show similar segmentation results. To validate this concept, we conducted a follow-up experiment. Figure 9 shows six sequential images (in depth) taken by the confocal microscope of the marked Golgi apparatus. In fact, the image shown in Figure 5 was cropped from this set of images. Therefore, the segmentation target inside these six images should be similar to that of the previous experiment. We implemented an automatic segmentation of these six images by using the same 10 algorithms shown in Table 1. The target region (the Golgi apparatus) was clearly correctly segmented from these very noisy images in A4, A5, A6, A9, and A10 (Fig. 10). However, A9 and A10 made a crucial mistake in the number of segmented regions because target regions overlapped each other, whereas

A4, A5, and A6 achieved an accurate segmentation. The cell biologist who provided the ground-truth evaluated the result from A4 and determined that the selection result of this algorithm was correct.

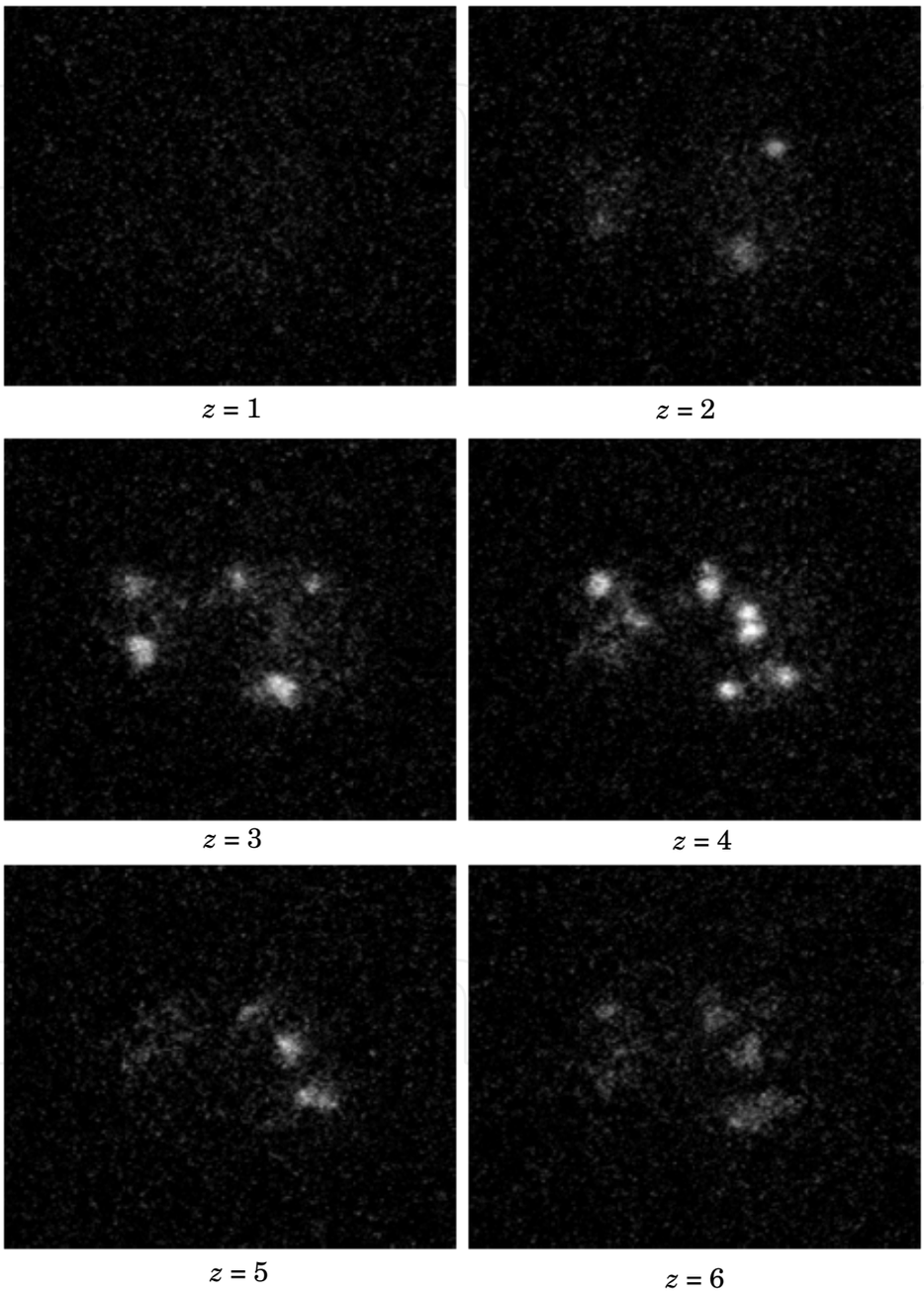

Fig. 9. Live-cell images of botanical yeast with marked regions of the Golgi apparatus. z indicates the depth position of each image.

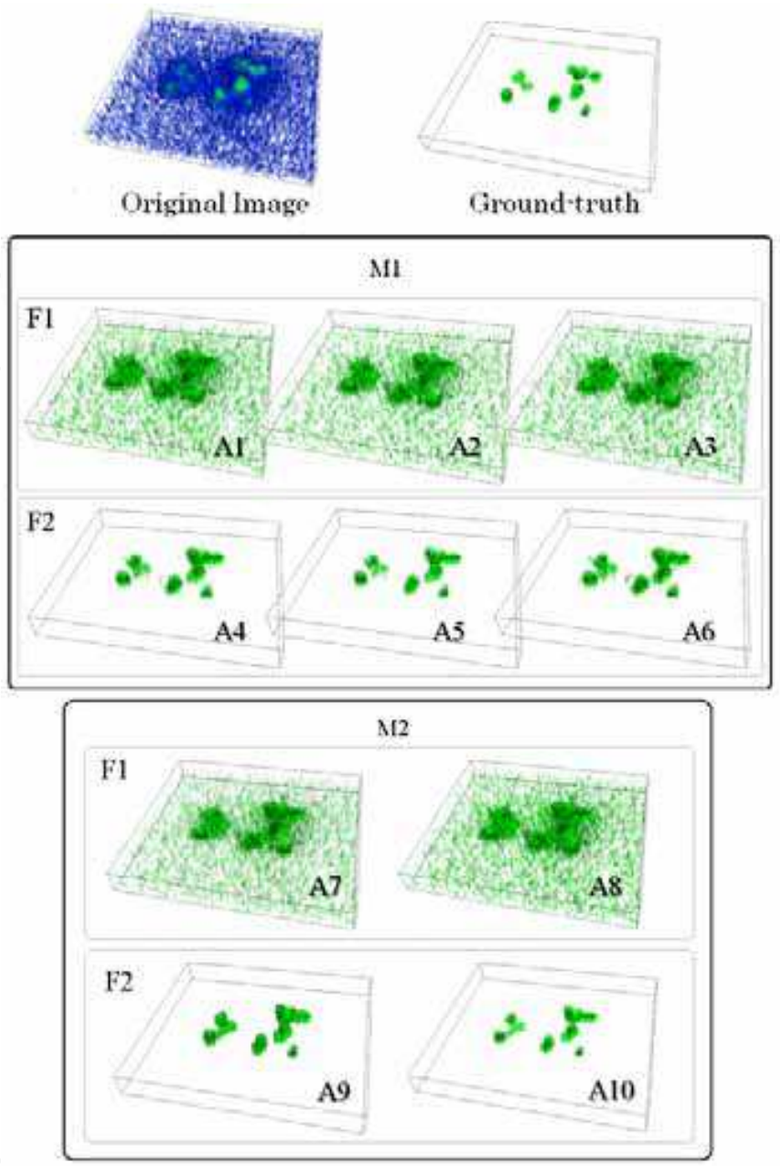

Fig. 10. Segmentation results of botanical yeast from multi-slice images. The green region in the ground-truth image shows the target region for segmentation.

4. Conclusion

We have proposed a novel framework for intracellular image segmentation based on effective algorithm selection. Selection is conducted by measurement both of similarities of intensity-based image features and of boundary shape between the user-supervised region and the automatically segmented regions generated by the given pattern classification techniques. Our framework assumes that the algorithm, which has powerful segmentation ability for a test image, will show good segmentation results for other similar images. That is, our framework can select an optimal algorithm to segment a region that has similar characteristics to the user-supervised region, even from many images. Furthermore, as

shown in the experiment, our framework can rank different algorithms and define the parameters of each algorithm.

The evaluation function presented here is versatile, but further investigation may reveal other functions that are better able to reflect a user's intention. In addition, our framework needs to be expanded to be able to better represent image features and boundary shape, and it should include more classification rules and a greater variety of parameters. We tested only two types of features and two types of classification rules as a prototype framework. These types of improvements will lead to segmentation that will have the necessary generality to conduct the variety of segmentation tasks required by researchers. As a result, we believe that researchers will be released from a labour-intensive and troublesome task and able to concentrate on the accumulation of valuable data.

5. Acknowledgements

This work was supported in part by Strategic Programs for R&D (President's Discretionary Fund) of RIKEN and Grants-in-Aid for Scientific Research of Japan (19800062 and 20113007). The cell images were taken at the Molecular Membrane Biology Laboratory of RIKEN. Part of the results of the calculations was performed by using the RIKEN Super Combined Cluster (RSCC) system and the RIKEN Integrated Cluster of Clusters (RICC) system.

6. References

Arbelaez, P.; Maire, M.; Fowlkes, C. & Malik, J. (2009). From contours to regions: An empirical evaluation. *Proceedings of IEEE Computer Society Conference on Computer Vision and Pattern Recognition*, pp. 2294-2301, ISBN: 978-1-4244-3992-8, Miami, USA, June 2009.

Arya, S.; Mount, D.M.; Netanyahu, N.S.; Silverman, R. & Wu, A.Y. (1998). An optimal algorithm for approximate nearest neighbor searching in fixed dimensions. *Journal of the ACM,* 34, 6, pp. 891-923.

Bhaskar, H. & Singh, S. (2007). Live cell imaging: a computational perspective. *Journal of Real-Time Image Processing*, 1, pp. 195–212.

Cardoso, J.S. & Corte-Real, L. (2005). Toward a generic evaluation of image segmentation. *IEEE Transactions on Image Processing*, 14, 11, pp. 1773–1782, ISSN: 1057-7149.

Cong, G. & Parvin, B. (2000). Model-based segmentation of nuclei. *Pattern Recognition*, 33, 8, pp. 1383-1393.

Duda, R. O.; Stork, D. G. & Hart, P. E. (2000). *Pattern Classification (2nd edition)*, Wiley-Interscience, ISBN: 978-047105669-0, New York.

Eils, R. & Athale, C. (2003). Computational imaging in cell biology. *The Journal of Cell Biology*, 161, 3, May 2003, pp. 477-481.

Goldman, R.D. & Spector, D. L. (2004). Live Cell Imaging: A Laboratory Manual, *Cold Spring Harbor Laboratory Press*, ISBN: 978-087969683-2.

Haindl, M. & Mikes, S. (2008). Texture segmentation benchmark. *Proceedings of the 19th International Conference on Pattern Recognition*, Los Alamitos, December 2008, pp. 1-4.

Haralick. R.M. & Shapiro, L.G. (1985). Survey: Image segmentation techniques. *Computer Vision, Graphics, and Image Processing*, 29, pp. 100–132.

Harder, N.; Eils, R. & Rohr, K. (2008). Automated classification of mitotic phenotypes of human cells using fluorescent proteins. *Methods in Cell Biology*, 85, pp. 539–554.

Jiang, X.; Marti, C.; Irniger, C. & Bunke, H. (2006). Distance measures for image segmentation evaluation. *EURASIP Journal on Applied Signal Processing*, 35909, pp. 1-10, ISSN:1110-8657.

Levine, M.D. & Nazif, A.M. (1985). Dynamic measurement of computer generated image segmentation. *IEEE Transaction on Pattern Analysis and Machine Intelligence*, 7, 2, pp. 155-164, ISSN: 0162-8828

Martin, D.; Fowlkes, C.; Tal, D. & Malik, J. (2001). A database of human segmented natural images and its application to evaluating segmentation algorithms and measuring ecological statistics. *Proceedings of IEEE International Conference on Computer Vision*, 2, pp. 416–423, ISBN: 0-7695-1143-0, Vancouver, July 2001.

Otsu, N. (1979). A threshold selection method from gray-level histograms. *IEEE Transaction on Systems, Man and Cybernetics*, 9, pp. 62–66.

Pal, N.R. & Pal, S.K. (1993). A review on image segmentation techniques. *Pattern Recognition*, 26, 9, pp. 1277–1294.

Polak, M.; Zhang, H. & Pi, M. (2009). An evaluation metric for image segmentation of multiple objects. *Image and Vision Computing*, 27, 8, pp. 1223-1227.

Sahoo, P.K.; Soltani, S. & Wang, A.K.C. (1988). A survey of thresholding techniques. *Computer Vision, Graphics, and Image Processing*, 41, 2, pp. 233-260, ISSN:0734-189X.

Sekita, I.; Kurita, T. & Otsu, N. (1992). Complex autoregressive model for shape recognition. *IEEE Transactions on Pattern Analysis and Machine Intelligence*, 14, 4, pp. 489–496.

Vapnik, V.N. (1995). The Nature of Statistical Learning Theory, Springer Verlag, ISBN: 978-038794559-0, New York.

Unnikrishnan, R.; Pantofaru, C. & Hebert, M. (2007). Toward objective evaluation of image segmentation algorithms. *IEEE Transaction on Pattern Analysis and Machine Intelligence*, 29, 6, pp. 929-944.

Waltera, T.; Helda, M.; Neumanna, B.; Hérichéb, J.K.; Conrada, C.; Pepperkoka, R. & Ellenberga, J. (2010). Automatic identification and clustering of chromosome phenotypes in a genome wide RNAi screen by time-lapse imaging, *Journal of Structural Biology*, 170, 1, pp. 1-9.

Yasnoff, W.A.; Mui, J.K. & Bacus, J.W. (1977). Error measures for scene segmentation, *Pattern Recognition*, 9, 4, pp. 217-231.

Zhang, H.; Cholleti, S.R.; Goldman, S.A. & Fritts, J.E. (2006). Meta-Evaluation of Image Segmentation Using Machine Learning. *Proceedings of IEEE Computer Society Conference on Computer Vision and Pattern Recognition*, 1, pp. 1138-1145, New York, June 2006.

Zhang, H.; Fritts, J.E. & Goldman, S.A. (2008). Image segmentation evaluation: A survey of unsupervised methods. *Computer Vision and Image Understanding,* 110, 2, pp. 260-280, ISSN:1077-3142.

Zhang, Y.J. & Gerbrands, J.J. (1992). Segmentation evaluation using ultimate measurement accuracy. *Proceedings of SPIE*, 1657, pp. 449–460, Image Processing Algorithms and Techniques III, ISBN: 9780819408112 , May 1992.

Zhang, Y.J. (1996). A survey on evaluation methods for image segmentation. *Pattern Recognition*, 29, 8, pp. 1335–1346.

Zhang, Y.J. (2006). *Advances in Image and Video Segmentation*, IRM Press, ISBN: 978-159140753-9, USA.

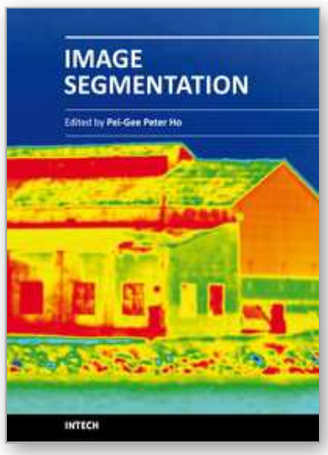

Image Segmentation
Edited by Dr. Pei-Gee Ho

ISBN 978-953-307-228-9
Hard cover, 538 pages
Publisher InTech
Published online 19, April, 2011
Published in print edition April, 2011

It was estimated that 80% of the information received by human is visual. Image processing is evolving fast and continually. During the past 10 years, there has been a significant research increase in image segmentation. To study a specific object in an image, its boundary can be highlighted by an image segmentation procedure. The objective of the image segmentation is to simplify the representation of pictures into meaningful information by partitioning into image regions. Image segmentation is a technique to locate certain objects or boundaries within an image. There are many algorithms and techniques have been developed to solve image segmentation problems, the research topics in this book such as level set, active contour, AR time series image modeling, Support Vector Machines, Pixon based image segmentations, region similarity metric based technique, statistical ANN and JSEG algorithm were written in details. This book brings together many different aspects of the current research on several fields associated to digital image segmentation. Four parts allowed gathering the 27 chapters around the following topics: Survey of Image Segmentation Algorithms, Image Segmentation methods, Image Segmentation Applications and Hardware Implementation. The readers will find the contents in this book enjoyable and get many helpful ideas and overviews on their own study.

INTECH
open science | open minds

InTech Europe
University Campus STeP Ri
Slavka Krautzeka 83/A
51000 Rijeka, Croatia
Phone: +385 (51) 770 447
Fax: +385 (51) 686 166
www.intechopen.com

InTech China
Unit 405, Office Block, Hotel Equatorial Shanghai
No.65, Yan An Road (West), Shanghai, 200040, China
中国上海市延安西路65号上海国际贵都大饭店办公楼405单元
Phone: +86-21-62489820
Fax: +86-21-62489821

IntechOpen